

The Three-Dimensional Structure of a Sunspot Magnetic Field

H. Socas-Navarro

High Altitude Observatory, NCAR¹, 3450 Mitchell Lane, Boulder, CO 80307-3000, USA

navarro@ucar.edu

ABSTRACT

Here we report on observations of the three-dimensional structure of a sunspot magnetic field from the photosphere to the chromosphere, obtained with the new visible/infrared spectro-polarimeter SPINOR. The observations, interpreted with a non-LTE modeling technique, reveal a surprisingly complex topology with areas of opposite-sign torsion, suggesting that flux-ropes of opposite helicities may coexist together in the same spot.

Subject headings: line: profiles – Sun: atmosphere – Sun: magnetic fields – Sun: chromosphere

The observations that we used in this work are first-light data from the new instrument SPINOR (Spectro-Polarimeter for INfrared and Optical Regions, Socas-Navarro et al. 2005). Still under development, SPINOR can already be used for high-resolution full spectro-polarimetry at virtually any combination of 3 spectral regions in the 400 - 1000 nm range. The particular dataset that we report on was acquired on 16 June 2004 at 15:16 UT. We observed two photospheric Fe I lines (at 849.7 and 853.8 nm) and two chromospheric lines of the Ca II infrared triplet (at 849.8 and 854.2 nm) in active region NOAA 0634 at a time of particularly good seeing. The spectrograph slit was scanned over that region to construct a three-dimensional datacube, in such a way that for each (x,y,λ) point we have the four Stokes parameters I, Q, U and V . We made use of the new adaptive optics system (Ren et al. 2003) of the Dunn Solar Telescope. Combined with the excellent atmospheric conditions at the time of the observations, we achieved a spatial resolution as good as 0.6" (note that this figure varies slightly in the scanning direction due to temporal changes in the seeing conditions), which is among the best attained thus far in this kind of observations.

¹The National Center for Atmospheric Research (NCAR) is sponsored by the National Science Foundation.

The sunspot subject to detailed analysis is rather irregular (see Fig 1) and exhibits two distinct umbral cores adjacent to the main umbra. One of them, above the main umbra in the figure, is surrounded by its own penumbra. The other umbral core is almost merged with the main umbra and is seen to its left separated by a faint light bridge. The interpretation of the data was done using the Stokes inversion code developed by Socas-Navarro et al. (2000) for spectral lines formed in non-LTE. The code infers the depth stratification of the temperature, line-of-sight velocity and magnetic field vector that yields the best fit to a particular set of Stokes spectra. The photospheric Fe blends in the wings of the Ca lines are also computed by the code, providing a fully connected picture of the whole atmosphere from the low photosphere to the chromosphere.

Each spatial point in the dataset is analyzed independently of the rest. In order to ensure proper convergence and minimize the risk of the algorithm settling in secondary minima, each inversion is repeated 10 times with randomized initializations. The best solution is picked as representative of the atmospheric conditions in the spatial location under study. The non-LTE inversions are very computing-intensive. However, this kind of analysis is necessary for accurate vector magnetometry (Lites et al. 1994; Socas-Navarro 2002) because radiative transfer and magneto-optical effects give rise to very complex dependences of the observables on the atmospheric conditions. We employed a scheme by which the non-LTE inversion code is efficiently run in parallel on several networked workstations. The hardware employed includes three dedicated and three shared (mostly off-hours) Intel P4 processors running Linux kernels. On average, we used the equivalent of 5 processors running at a clockspeed of 2.7 GHz. The real-time employed in the entire analysis was 29 days. This included a first inversion of a larger area (some 200x150 pixels) and a second pass at the area framed by a rectangle in Figure 1, of nearly 150x110 pixels. In the second pass, the profiles were averaged over a 3x3 pixel (1.1"x0.66") box before inverting with the aim of improving the signal-to-noise ratio. The noise level was thus reduced to approximately 1.5×10^{-4} in units of the quiet Sun continuum intensity.

The detailed analysis outlined above produced a 3D reconstruction of the full magnetic field vector in the active region. Figure 1 shows the magnetic structure in the large sunspot, after deprojecting it to disk center and with the magnetic field transformed to the solar reference frame. The 180-degree ambiguity in the (observer frame) azimuth was resolved by picking the value that results in a more radial field when converted to the solar coordinate frame. As a consistency test, we computed the divergence of the field across the entire map using boxes of 1.6 Mm in each dimension. It was found that the divergence is always small compared to B/l (the magnitude of the field divided by the length of the box), with an average absolute value of 1.8%. This argument, as well as the spatial coherence of the results obtained (recall that each pixel was inverted independently), strongly supports the

reliability of our findings.

The east side of the sunspot (left of the figure) is reminiscent of what is typically found in numerical simulations of a simple sunspot, with field lines bending outwards in the penumbra. This area is partly force-free, as can be deduced from Fig 2 (recall that the condition for a force-free field is that $\nabla \times \vec{B}$ must be parallel or anti-parallel to \vec{B}), particularly in the chromosphere, but not entirely. The west side (right of the figure), on the other hand, exhibits a very different structure and the field is mostly non-force-free. Photospheric magnetograms of the region (not show in the figures) reveal an intricate pattern of flux near the sunspot on that side, suggesting a complex topology that would manifest itself also in the sunspot structure, perturbing the field away from the classical picture of a near-potential configuration. This idea is further supported by H_α images from the same day (e.g., Active Region Monitor at NASA Goddard Space Flight Center’s Solar Data Analysis Center: <http://www.solarmonitor.org/20040616/0634.html>) showing considerable activity on the west side of this sunspot.

To avoid confusion with the terminology, which is sometimes used with different meanings in the literature, we adopt the following definitions in this work. We denote by ”twist” the deviation of the field from the radial direction and by ”torsion” the vertical gradient of the azimuth². In this context, the concept of torsion is probably better defined from a mathematical point of view because the radial direction is not well defined in cases like the present one. Furthermore, while twist and torsion (as defined here) refer essentially to the same concept in a rigid object, this is not necessarily the case in non-rigid systems such as the magnetic field lines. Imagine, for example, a magnetic field that does not vary along the flux-rope axis but whose azimuth does not follow the radial direction. This configuration would have twist but not torsion. A detailed representation of the magnetic torsion is provided in Fig 3. This figure shows that the torsion is negative over most of the sunspot, but there are also two large areas of positive torsion. The first one corresponds roughly to the upper-right quadrant. It may be associated with the direction connecting the main umbra to the umbral core located towards the north-west. The torsion in this area decreases in magnitude as we move up into the chromosphere. The other positive-torsion area is roughly the lower-left quadrant and, contrarily to the first one, its magnitude increases with height.

The results presented in this paper reveal a very complex topology of sunspot fields. The fact that most of the spot departs from the force-free regime is quite surprising and has some important implications. While the force-free approximation is a convenient way to

²The term azimuth here is defined as the angle between the (measured) magnetic field vector \vec{B} and the solar East-West direction, measured counter-clockwise from the solar West.

estimate the magnetic field structure (whether by means of extrapolations or using it to make empirical twist determinations), our observations do not support its applicability in general. Empirical determinations of twist or electric currents from 2D maps in complex regions seem particularly questionable. In fact, such investigations have even more caveats because one can only obtain one of the components of the curl vector and also because the "measurement heights" at different pixels have variations as large as 500 km in a sunspot. In summary, there are no convenient shortcuts to measuring the actual 3D structure of the field via full Stokes spectro-polarimetry and proper non-LTE modelling. Finally, it is important to note that the non-force-freeness of the field provides potential energy that may become available for chromospheric/coronal heating by means of magnetic reconnection into a lower energy state. The coexistence of opposite-sign torsions is a rather surprising finding since, to the author's best knowledge, it has not been predicted or proposed in any previous theoretical models.

The physical mechanism that twists the field is yet to be established. Three different processes have been proposed: a) the dynamo itself generates twisted fields (Choudhuri et al. 2004); b) Coriolis forces twist the flux-tubes during their ascent (Fisher et al. 2000; Fan & Gong 2000); c) turbulent convective buffeting twists the flux-tubes during their travel through the convection zone (Longcope et al. 1998). The mixed-twist scenario of our observations seems to be difficult to explain by the first two possibilities, which should produce flux-ropes of the same sign twist in a given active region. The convective buffeting scenario, on the other hand, is essentially a turbulent process and would naturally produce either sign twist in a more or less stochastic manner. Therefore, while the three mechanisms are probably contributing with different relative importance, our data indicates that the convective buffeting is probably the dominant one. However, convective buffeting cannot be the only mechanism for producing twist, since the statistics of active regions clearly indicate that there is also a systematic trend in the twist (see, for example, Pevtsov et al. 1995).

REFERENCES

- Choudhuri, A. R., Chatterjee, P., & Nandy, D. 2004, ApJ, 615, L57
- Fan, Y., & Gong, D. 2000, Solar Phys., 192, 141
- Fisher, G. H., Fan, Y., Longcope, D. W., Linton, M. G., & Pevtsov, A. A. 2000, Solar Phys., 192, 119
- Lites, B., Martínez Pillet, V., & Skumanich, A. 1994, Sol. Phys., 155, 1
- Longcope, D. W., Fisher, G. H., & Pevtsov, A. A. 1998, ApJ, 507, 417
- Pevtsov, A. A., Canfield, R. C., & Metcalf, T. R. 1995, ApJ, 440, L109
- Ren, D., Hegwer, S. L., Rimmele, T., Didkovsky, L. V., & Goode, P. R. 2003, in Innovative Telescopes and Instrumentation for Solar Astrophysics. Edited by Stephen L. Keil, Sergey V. Avakyan . Proceedings of the SPIE, Volume 4853, pp. 593-599 (2003).., 593–599
- Socas-Navarro, H. 2002, in SOLMAG 2002. Proceedings of the Magnetic Coupling of the Solar Atmosphere Euroconference and IAU Colloquium 188, 11 - 15 June 2002, Santorini, Greece. Ed. H. Sawaya-Lacoste. ESA SP-505. Noordwijk, Netherlands: ESA Publications Division, ISBN 92-9092-815-8, 2002, p. 45 - 51, 45
- Socas-Navarro, H., Elmore, D., Pietarila, A., Darnell, T., Tomczyk, S., & Lites, B. 2005, Solar Physics, *submitted*
- Socas-Navarro, H., Trujillo Bueno, J., & Ruiz Cobo, B. 2000, ApJ, 530, 977

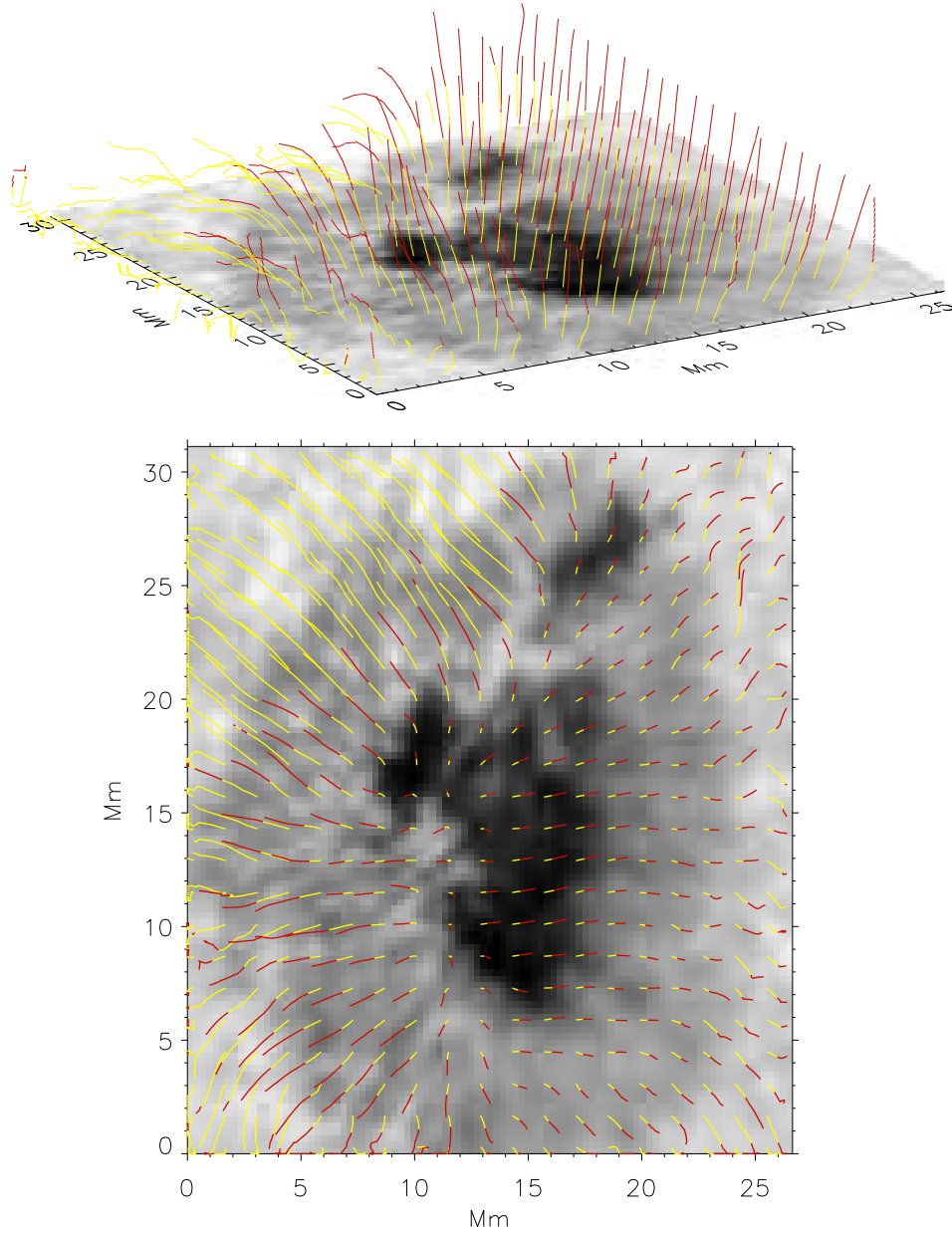


Fig. 1.— Three-dimensional structure of the magnetic field lines. Upper panel: Perspective view. Lower panel: Top view. The height range between 0 and 800 km is represented in yellow, whereas the range between 800 and 1600 km is in red. Axes are in megameters (Mm). Only field lines originating on a 5×5 (5×10) pixel grid are shown in the lower (upper) panel to avoid cluttering the figure.

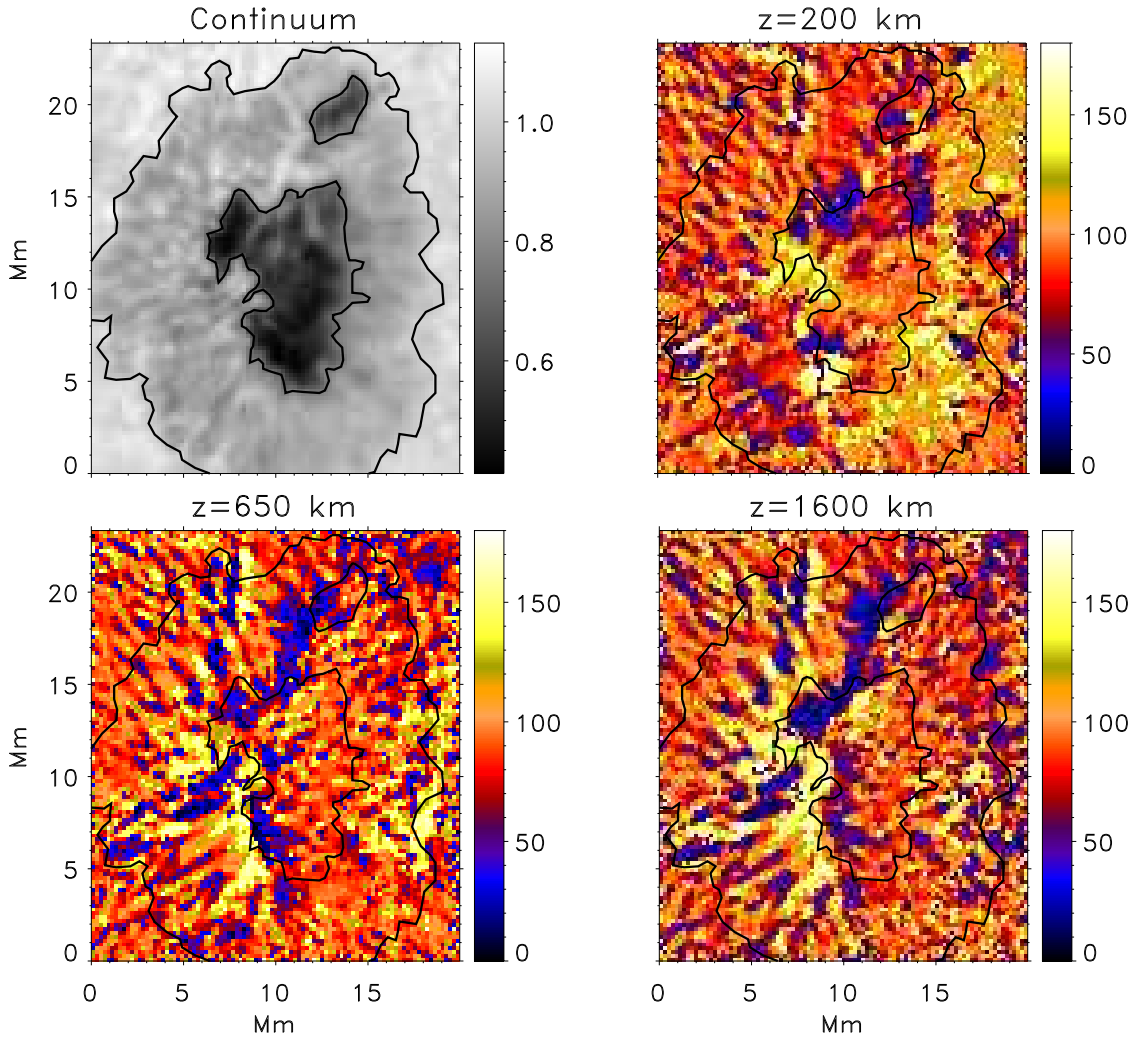


Fig. 2.— Maps of the angle between vectors $\nabla \times \vec{B}$ and \vec{B} at three different heights. The field is strictly force-free only in those pixels shown in dark blue (parallel) or light yellow (anti-parallel) colors.

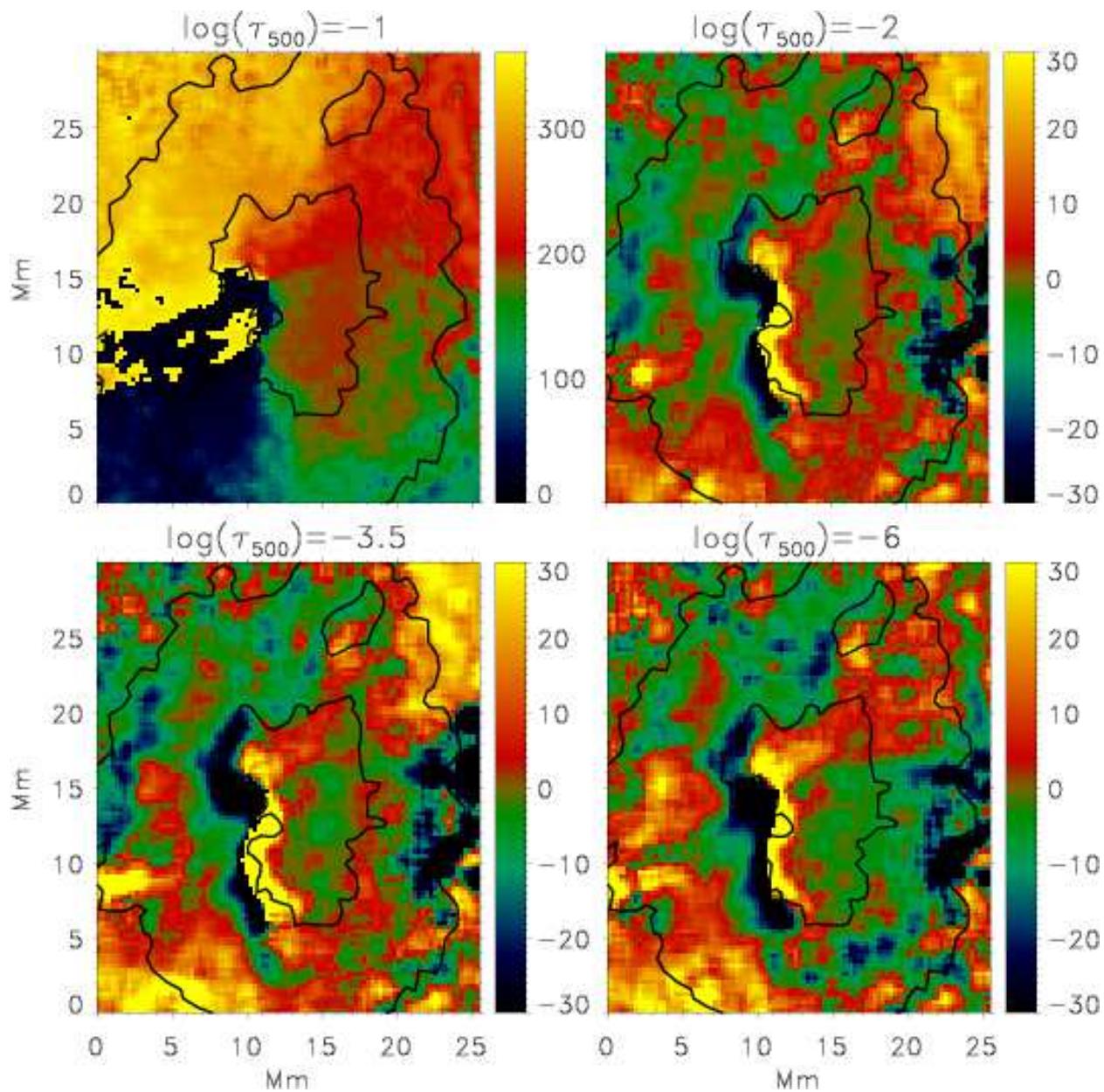


Fig. 3.— Torsion maps. The color scale represents degrees measured counter-clockwise from the solar west direction. The upper-left panel shows the photospheric azimuth. All other panels show the difference between the azimuth at optical depth indicated by the label minus the photospheric azimuth (shown in the first panel), i.e. the magnetic torsion. The umbral and penumbral boundaries are overlaid for reference.